Heliyon 10 (2024) e32920

Contents lists available at ScienceDirect

Heliyon

journal homepage: www.cell.com/heliyon

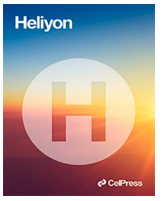

Research article

Historical sedimentary and evolutionary characteristics of POPs and EDCs in typical regions of the three Gorges reservoir, China

Lei Dong [a,b,c], Yueqi Cao [a,b], Xiong Pan [a,b,c], Li Lin [a,b,c,*], Xiaohe Luo [d], Nima Dunzhu [d], Jiancheng Hu [e]

[a] Basin Water Environmental Research Department, Changjiang River Scientific Research Institute, Wuhan, 430010, PR China
[b] Key Lab of Basin Water Resource and Eco-Environmental Science in Hubei Province, Wuhan, 430010, PR China
[c] Innovation Team for Basin Water Environmental Protection and Governance of Changjiang Water Resources Commission, Wuhan, 430010, PR China
[d] The Resettlement Affairs Center for Large and Medium-Sized Water Conservancy and Hydropower Projects in Xizang Autonomous Region, Lhasa 850000, P.R. China
[e] School of Environmental Studies, Hubei Polytechnic University, Huangshi 435003, P.R. China

ARTICLE INFO

Keywords:
Three Gorges reservoir
POPs
EDCs
Sediment core
Vertical distribution
Historical deposition

ABSTRACT

The historical sedimentary and evolutionary characteristics of persistent organic pollutants and endocrine disruptors in typical regions of the Three Gorges Reservoir are scarcely studied. Herein, the 96-year data on contaminated sediment history were reconstructed using Caesium 137 isotope dating. Polychlorinated biphenyl concentrations in the involved sediment cores ranged from non-detected (ND) to 11.39 ng/g. The concentrations of polycyclic aromatic hydrocarbons ranged from ND to 2075.20 ng/g and peaked in the 1970s owing to natural, agricultural and human activities. Further, phthalate esters (PAEs) and heavy metals (HMs) were detected at concentrations ranging from ND to 589.2 ng/g and 12.10–93.67 μg/g, respectively, with highest values recorded in the 1980s owing to rapid industrialisation and insufficient management during China's early reform and development stages. PAE and HM concentrations have increased in recent years, suggesting the need to focus on industrial and agricultural activities that have caused this impact. Although current pollutant concentrations in sediments do not pose a risk to the aquatic ecosystem, they should be continuously monitored.

1. Introduction

Persistent organic pollutants (POPs), including polycyclic aromatic hydrocarbons (PAHs), polychlorinated biphenyls (PCBs) and organochlorine pesticides (OCPs), accumulate via food webs and adversely affect human health and the environment [1–3]. Endocrine disrupting chemicals (EDCs), including phthalates (PAEs) and heavy metals (HMs) such as lead (Pb), cadmium (Cd) and mercury (Hg), are exogenous compounds that can interfere with the endocrine systems of humans and animals, thus adversely affecting them and their offspring [4]. POPs and EDCs are partly produced via incomplete combustion of natural organic substances and human activities [5].

* Corresponding author. Basin Water Environmental Research Department, Changjiang River Scientific Research Institute, Wuhan, 430010, PR China.
E-mail address: linli1229@hotmail.com (L. Lin).

https://doi.org/10.1016/j.heliyon.2024.e32920
Received 15 March 2024; Received in revised form 2 May 2024; Accepted 12 June 2024
Available online 13 June 2024

Sediments are crucial in the circulation, transfer and storage of these pollutants in aquatic ecosystems, acting as both a sink and source [6]. Caesium 137 (^{137}Cs)—an artificial radionuclide produced during nuclear weapon testing—is widely used for sediment dating [7]. Yang et al. used ^{210}Pb, ^{226}Ra and ^{137}Cs to measure the concentration and deposition flux of PAHs and indicated an increase in the contribution of anthropogenic sources from the bottom to the top of sediment cores in the East Lake in Wuhan [8]. Singh et al. established a temporal sequence of sediment cores via ^{137}Cs analysis, studied the sediment accumulation rate in India's Lake Pikala and estimated that Lake Pikala existed for approximately 514.08 years [9]. Zhou et al. measured polychlorinated dibenzo-p-dioxins (PCDDs) and polychlorinated dibenzofurans (PCDFs) in sediment cores obtained from Xiangxi River, a tributary of the Three Gorges, using ^{137}Cs and ^{210}Pb radionuclides. They found higher concentrations of PCDDs and PCDFs in 1960–1990 compared with those in other years, confirming remarkable differences in each sediment layer [10]. Current studies primarily focus on dating sediment cores in shallow lakes and rivers and analysing the corresponding typical pollutant concentration and distribution. Compared with those corresponding to shallow lakes and rivers, the flow velocities in front of reservoir dams are lesser owing to dam interception. Moreover, sediments have a higher deposition rate; therefore, reservoirs are commonly regarded as the primary origin of and accumulation sites for POPs and EDCs in the natural environment [11]. Indicators such as total nitrogen, ^{210}Pb and ^{137}Cs have been previously used to assess nutrient sources and reservoir sedimentation rates [12,13]. However, the historical deposition and evolution of pollutants in large deep-water reservoir sediments are scarcely studied because of sampling constraints and harsh conditions.

The Three Gorges Reservoir (TGR) is the world's largest water conservancy project with a dam height of 181 m and storage capacity of 3.93×10^{10} m^3 [14]. The condition of the water environment in the Three Gorges region of the Yangtze River directly influences the ecological environments of the basin and the adjacent coastline. The quality and stability of the water environment determine the extent of biodiversity, the health status of aquatic ecosystems, and the stability of surrounding ecosystems in this area. Consequently, maintaining the favorable condition of the water environment in the Three Gorges region is of paramount importance for preserving basin ecological equilibrium and ensuring coastal ecological security. Wang et al. found that the PAHs concentrations varied from 13.8 to 97.2 ng/L, primarily in the upper reaches of the dam and in regions around the dam; the pCB levels ranged from 0.08 to 0.51 ng/L, with the highest concentration near the dam, whereas OCPs were more uniformly distributed at 2.3–3.60 ng/L in the TGR water bodies [15]. Lin et al. found higher concentrations of PAHs and PAEs in surface water and sediments during impoundment compared to discharge periods [16]. Floehr et al. confirmed PAHs as the primary pollutants in the TGR that caused genetic toxicity damage to fish [17]. However, the historical deposition and evolution characteristics of pollutants such as POPs and EDCs in TGR sediments and their environmental impact have not been reported yet but are crucial for water environment management and optimal TGR dispatching plans.

This study aimed to analyse sediment samples from representative locations in the TGR to reconstruct historical pollution levels and assess the environmental quality. To this end, the ^{137}Cs isotope was considered to analyse the dating of sediment cores, and the occurrence characteristics and chronological vertical-distribution patterns of POPs and EDCs were studied. Moreover, the sources and primary environmental factors of POPs and EDCs were analysed, and ecological risk assessment of sediment was performed. Overall, this study can provide valuable insights for analysing the accumulation characteristics of the sediment in front of large reservoir dams, vertical-distribution characteristics of sediment POPs and EDCs and associated ecological risks. This research provides essential data and technical support for the operational management of large-scale hydraulic engineering projects and the management of POPs and EDCs.

Fig. 1. Sampling sites in the TGR during the low-water-level operation period.

2. Materials and methods

2.1. Research area

The TGR is approximately 760-km long and 1.1-km wide, with a total area of 1080 km^2; it has a water storage capacity of approximately 400×10^8 m^3, making it the largest water conservancy and hydropower project globally [18]. The operational timeline of the TGR can be categorised into four water periods: impoundment (September–October), high-water-level operation (November–April), discharge (May–June) and low-water-level operation (June–August) [19]. Although the exact durations of these periods may vary slightly each year, the water level remains relatively stable at 145 m from June to August. In September–October, the water level in the reservoir gradually increases from 145 to 156 m and then rapidly increases to approximately 175 m. From November to the end of April of the following year, the reservoir consistently maintains a high water level. Commencing in May, the water level within the reservoir area starts decreasing, reaching 145 m by early June [20].

2.2. Monitoring location and sample collection

The Bureau of Hydrology, Changjiang Water Resources Commission, published the hydrology and sediment deposition monitoring results of the TGR for a long time series. Based on their report, five sampling sites were established in August 2022 (during low-water-level operation) to study the distribution characteristics of pollutants in the surface sediments in four typical siltation regions: Fuling (FL, S1), Zhongxian (ZX, S2), Fengjie (FJ, S3) and Zigui (ZG, S4) in the TGR and Baixia (BX, S5) in the vicinity of the underground power plant on the right bank of the Three Gorges Power Station under the dam. The layout of the sections and their latitudes and longitudes are presented in Fig. 1 and Table S1, respectively. FL, ZX, FJ, ZG and BX are ~392, 296, 148, 5 and 6 km away from the Three Gorges Dam, respectively. The surface sediment was collected using a grab sampler.

Columnar sediment samples were collected using a shipboard geological exploration core drill rig (Fig. 1). Columnar sediments were drilled up to the riverbed rock layer in Zigui (S4), with a sampling depth of 23 m. Sediment cores were collected using a stainless-steel pipe with a pre-installed diameter of 10 cm. A total of 23 columnar samples were collected (1 m in length), where the corresponding depth ranges of the first and last columnar samples were 0.0–1.0 and 22.0–23.0 m, respectively. For ^{137}Cs dating analysis, 23 sampling points (Z1–Z23) were set vertically and the cross-section was divided into one layer every 1.0 m. Specific sampling points corresponding to the vertical depth are shown in Table S2. The surface and columnar sediment samples were stored in a refrigerator at 0°C-4°C and transferred to the laboratory for further analysis, where they were stored at −20 °C. Detailed analysis of the conventional physicochemical parameters and HMs is given in Text S1, Supplementary material.

The pre-treated sediment core samples were analysed using a high-purity germanium gamma-ray spectrometer (GEM–C7080–LB–C, ORTEC, USA). The peak area corresponding to a^{137}Cs gamma energy of 661.6 keV (85 %) in the energy spectrum was calculated. Specific analysis sediment dating using ^{137}Cs is described in Text S2, Supplementary material.

2.3. POP and PAE analyses

The chemicals and reagents used herein are detailed in Text S3, Supplementary material. Ultrapure water was obtained using an ultrapure-water system (Milli-Q Direct 8, Millipore, USA). OCPs, PCBs, PAHs and PAEs were separated, identified and quantified through gas chromatography (Shimadzu, GC2010Plus), gas chromatography–mass spectrometry (Shimadzu, GCMS–QP2010SE) and gas chromatography–mass spectrometry (Aglent, 7890B/5977A), respectively. The specific extraction conditions and instrument analysis for POPs and PAEs in sediments are described, respectively, in Texts S4 and S5, Supplementary material.

2.4. Quality assurance and control

The quality assurance and control requirements for sample analysis adhered to the Regulation for Water Environmental Monitoring (SL–2013). The mixed-external-standard method was employed for the quantitative analysis of PCBs, OCPs, PAHs and PAEs in the samples. The correlation coefficients of the standard curves were all >0.99. After 10 consecutive sample analyses, the relative standard deviation from the initial concentration of the standard solution to the middle concentration point on the analysis curve was <15 %. The retest results of the concentration verification points in the middle of the analysis curve and the concentration results of the parallel samples met the requirements (<15 %). The limit of detection (LOD) was evaluated by calculating the signal-to-noise ratio three times. The LODs of 4 OCPs, 18 PCBs, 16 PAHs and 6 PAEs in sediments were 0.05–0.09, 0.03–0.14, 0.08–0.78 and 0.25–1.85 ng/g, respectively. By conducting recovery experiments wherein the corresponding standard solutions were added to the sediment samples, the recovery rates of 4 DDTs, 18 PCBs, 16 PAHs and 6 PAEs in the sediment were measured as 67.2%–103.2 %, 62.7%–96.7 %, 59.9%–80.7 % and 63.9%–75.5 %, respectively.

2.5. Data processing

All figures were drawn using Origin (version 2021), AutoCAD (version 2020) and ArcGIS (version 10.1). Distance–decay relationships (DDRs) were derived and variation partitioning analysis (VPA) was performed using the R programming language (Version 3.6.3); the specific operation process is presented in Text S6, Supplementary material. All samples were evaluated in triplicate, and the results were presented as the mean values. When calculating the concentrations of OCPs, PCBs, PAHs and PAEs, any data below the

LOD were considered non-detected (ND).

3. Results

3.1. Sediment characteristics

The average deposition rate of sediments in Zigui (S4) in front of the TGR dam was determined via isotope dating as 0.233 m/a, and the sediment core covered a time range from 1924 to 2019. The changes in the ^{137}Cs activity in the sediment core is shown in Fig. 2a. The distribution of organic matter (OM) in the sediment core is shown in Fig. 2b. The OM concentration in the sampling site was between 0.6 and 30.4 g/kg, with an average of 15.0 g/kg. The OM concentration showed a clear upward trend from 2002 to 2019, indicating that this period was considerably affected by human influence. The correlations between OM and different types of organic pollutants are discussed in subsequent sections.

3.2. Occurrence characteristics of POPs

3.2.1. DDTs

DDTs, the primary representative of OCPs, including *o,p*'-DDT, *p,p*'-DDD, *p,p*'-DDT and *p,p*'-DDE, were not detected in the surface sediments in Fuling (S1), Zhongxian (S2), Fengjie (S3) and Zigui (S4) in the TGR and the Baixia (S5) under the dam. DDTs were detected in the sediment core of Zigui (S4) in the range of ND–1.14 ng/g (Table S3). The correlation analysis results indicated that no statistically significant correlation was observed between DDT and OM concentrations, which was in line with previous research outcomes [21–23].

3.2.2. PCBs

PCBs were detected in the surface sediments in Fuling (S1), Zhongxian (S2), Fengjie (S3) and Zigui (S4) in the TGR. The concentrations of ∑PCBs were high in Fuling (S1, 2.16 ng/g), Fengjie (S3, 1.97 ng/g) and Zigui (S4, 1.83 ng/g), with the least value being in Baixia (S5, 0.09 ng/g) (Table S4). Previous study showed that sediments were sinks rather than secondary sources of PCBs [24]. PCBs resulting from dam construction as well as industrial and agricultural activities enter the reservoir through surface runoff and atmospheric sedimentation and are gradually deposited with sediments [25]. Consequently, the distribution of PCB concentrations was higher in the reservoir area than under the dam. These findings illustrated that the PCB concentrations in the four typical sections (S1–S4) of the TGR ranged from 0.75 to 2.16 ng/g; only PCB28 and PCB169 were detected therein. The PCB concentration was considerably lower in the TGR than those in densely populated and industrial areas, such as the Yangzte Estuary (1.86–148.22 ng/g) [26] and Zhoushan Islands (9.09–614.90 ng/g) [27].

The sediment core in Zigui (S4) was collected and PCB concentration was detected. Based on the data presented in Table S5, PCB169 and PCB52 emerged as the dominant contaminants in the sediment core, with concentrations of ND–8.18 ng/g (mean: 1.40 ng/g) and ND–6.27 ng/g (mean: 1.13 ng/g), respectively. The detection rates of PCB169 and PCB52 were >95 %, and those of other PCBs were <20 %. Moreover, PCB123, PCB118, PCB114, PCB126 and PCB189 were not detected. Correlation analysis revealed that ∑PCB and OM concentrations were not correlated.

3.2.3. PAHs

As shown in Table S6 and 16PAHs were detected in varying concentration in the surface sediment samples obtained from Fuling (S1), Zhongxian (S2), Fengjie (S3) and Zigui (S4) in the TGR, with the detection rate of 81.25%–100 %; the detection rate of samples in Zigui (S4) reached 100 %. However, a low concentration of PAHs was detected in Baixia (S5), namely Phe, Fla and Pyr, with a detection rate of 18.75 %. In the survey area, the PAH concentration ranged between 136.18 and 662.88 ng/g (mean: 408.57 ng/g) in the TGR. Notably, higher concentrations of Fla, Phe, BbF and Pyr were observed therein.

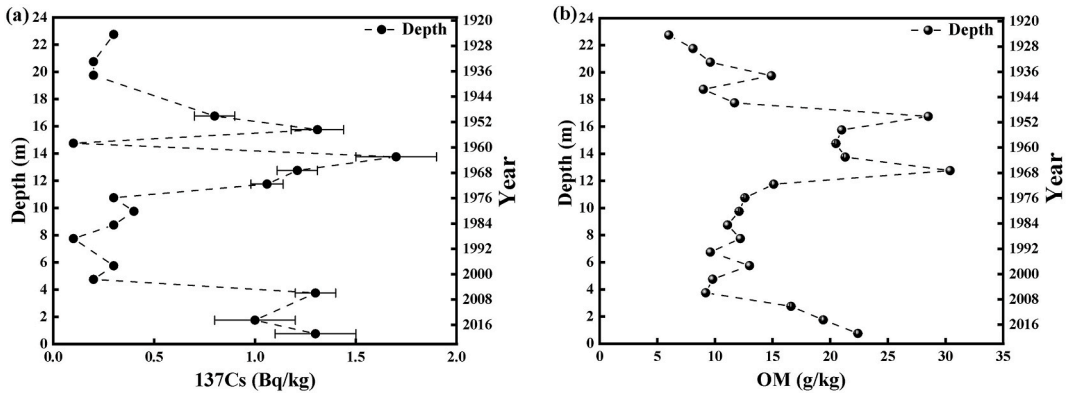

Fig. 2. ^{137}Cs specific activity (a) and OM dating distribution (b) in sediment cores.

PAH concentrations in the TGR were higher than those in the Manwan dam in the middle of Lancang River, China (14.4–137.7 ng/g, mean 71.51 ng/g) [28], Yuvacık Lake (36.97–81.38 ng/g) [29] and Itapicuru estuary (1.98–43.1 ng/g) [30]. These values were lower than the previously detected values for the Danjiangkou Reservoir area and Hanjiang River Basin, China (86.23–2514.93 ng/g, mean 365.43 ng/g) [31] as well as rivers, lakes and reservoirs in other parts of China, such as the Taihu Basin (26–5294 ng/g, mean 649 ng/g) [32], Fengshuba Reservoir (364.40–743.71 ng/g, mean 506.81 ng/g) [33] and Dahuofang Reservoir in Northeast China (323–912 ng/g, mean 592 ng/g) [34].

The PAH concentration in the reservoir area (S1–S4, average 408.57 ng/g) was significantly higher than under the dam (S5, mean 13.54 ng/g), possibly because of frequent human activities around the reservoir area. This caused the emission of PAHs from vehicle exhaust into the reservoir area via atmospheric deposition [35]. In addition, the flow velocity in the reservoir area was low, and PAHs easily settled and accumulated after sediment adsorption once they entered the water body [36]. Overall, PAH pollution was minimal in the TGR, indicative of good water quality.

The concentrations of PAHs in the sediment core are presented in Table S7. The detection rates of Phe, Fla, Pyr, BaA and Chr were the highest at 86.96 %. The concentration range of ∑PAHs was ND–295.84 ng/g (mean: 18.19 ng/g). The concentrations of 4–5-ring PAHs with high molecular weights, such as BbF, Fla and Pyr, were high, whereas those of 2–3-ring PAHs with low molecular weights, such as Nap, Ace and Acy, were low. This implied that 4–5-ring PAHs accounted for the largest proportion, 46.4 % and 24.5 %, respectively, whereas 2-ring PAHs accounted for the least, only 1.7 % (Fig. S1a). The involved vertical distribution (Z1–Z23) indicated that the distribution of 4-ring PAHs was the most extensive, and they were accumulated in all vertical sections, accounting for 28.32%–65.44 % (mean 38.53 %). However, 2-ring PAH concentrations were relatively low, accounting for ND–14.58 % (mean 4.52 %) (Fig. S1b). This is because PAHs with lower molecular weights, such as 2-ring PAHs, have high solubility in the aqueous phase, which decreases with biodegradation and volatilisation; in addition, PAHs with high molecular weights (4–5 rings) are easily adsorbed into sediments [37]. Correlation analysis revealed no significant correlation between PAHs and OM. However, a notable positive correlation was observed between PAHs and Pb ($r = 0.468$, $p < 0.05$), indicating that they may have the same source [38]. Furthermore, the coexistence of PAHs and Pb may cause greater genotoxicity to sediments [39], necessitating the monitoring of the ecological impact of their coexistence.

3.3. Occurrence characteristics of EDCs

3.3.1. PAEs

The detection results of PAEs in the TGR are presented in Table S8, with DBP and DEHP as major contributors. PEHP was detected in all sampling sites, whereas DBP was only distributed in Zigui (S4) and Fengjie (S3). The concentration of ∑PAEs in the reservoir area was 88.31–257.90 ng/g, with the highest value being in Fengjie (S3). Similar to the spatial distributions of PCBs and PAHs, the PAE concentration was considerably higher in the reservoir area (mean 167.53 ng/g) than under the dam (S5, 39.92 ng/g), possibly due to the interception of the dam and the discharge of domestic sewage and industrial wastewater [40]. The PAE concentrations in the surface sediments of the TGR were comparatively lower than those in other basins across China such as Haihe River (45.9–1474.1 ng/g) [41] and Jiaozhou Bay (462.1–15133.2 ng/g) [42].

Analysis of the PAE distribution in the sediment core (Table S9) revealed that the concentration of DEHP (mean: 127.6 ng/g) was generally higher than that of DBP (mean: 38.9 ng/g). Moreover, DEHP was detected in most samples, with detection rates of >90 %, indicating that it was more widely distributed. This finding agrees with those reported for Pearl River Delta, China [43]. The correlation analysis revealed no significant relationship between PAEs and OM, which aligns with the previously reported findings [43,44].

3.3.2. HMs

Three HMs were primarily detected in the reservoir area (Table S10)—cadmium (Cd), mercury (Hg) and lead (Pb). Cd, Hg and Pb were detected in all sampling sites, indicating that they were widely distributed. The total concentration of the three HMs (∑HMs) ranged from 34.18 to 68.87 μg/g, with a mean of 51.01 μg/g. The concentration of Pb was the highest, ranging from 34 to 68 μg/g, with a mean of 50.5 μg/g. The concentrations of ∑HMs in Zigui (S4) and Fuling (S1) were high, 68.87 and 62.70 μg/g, respectively, because these regions were densely populated, with good industrial and agricultural developments [45]. The concentration of HMs under the dam (S5) was 54.66 μg/g, which was close to that in the reservoir area. Overall, the concentrations of the three HMs in the reservoir area were in close agreement with the correlation values detected for the sediments in the TGR (mean values of 56.7 and 1.14 μg/g for Pb and Cd, respectively) [46] and Yangtze River Estuary (mean values of 30.47 ± 11.22, 0.15 ± 0.09 and 0.05 ± 0.02 μg/g for Pb, Cd and Hg) [47]. However, these values were slightly lower than those in other areas such as Dongting Lake (average concentrations of Pb, Cd and Hg were 54.82, 4.39 and 0.19 μg/g, respectively) [48] and Kallar Kahar Lake in Pakistan (mean concentrations of Cd and Pb were 0.59–0.89 and 7.6–18.6 μg/g, respectively) [49]. In summary, HM pollution was observed in the reservoir area.

In the sediment cores (Table S11), ∑HM concentration was ND–93 μg/g, with a mean of 16.12 μg/g. The concentrations of Cd, Hg and Pb were 0.09–1.43 μg/g (mean: 0.47 μg/g), ND–0.42 ng/g (mean: 0.09 μg/g) and 12–93 ng/g (mean: 47.79 μg/g), respectively. Thus, the concentration of Pb concentration was relatively higher, probably because it resulted from human activities. Correlation analysis revealed a significant correlation between ∑HMs and OM ($r = 0.671$; $p < 0.01$). The study indicated that OM could play a role in the complexation and chelation of HMs, influencing their migration, transformation and accumulation [50]. In particular, the concentrations of Hg and Pb were significantly correlated with that of OM ($r = 0.419$, $p < 0.05$; $r = 0.672$, $p < 0.01$, respectively), indicating that Hg and Pb were considerably affected by OM. In addition, Cd and Pb exhibited a strong significant correlation, indicative of their possible common source, i.e. industrial activities [51]. Moreover, the source of Hg could be agricultural activities [52].

4. Discussion

The majority of the TGR is situated within karst landforms, where rocky hills cover approximately 90 % of the area. The landscape type has changed from human-dominated farmland to naturally driven woodland and shrub land. The Jurassic red-bed sandstone on both banks constitutes an unstable slope [53]. The vertical-distribution patterns of pollution age, pollution sources, environmental factors and ecological risks of DDTs, PCBs, PAHs, PAEs and HMs are discussed herein.

4.1. Vertical-distribution pattern and source

4.1.1. POPs

(1) DDTs

DDTs are important OCPs, including *o,p*'-DDT, *p,p*'-DDD, *p,p*'-DDT and *p,p*'-DDE. Herein, only *p,p*'-DDE was detected in the concentration range of ND–1.14 ng/g, with a mean of 0.10 ng/g (Fig. 3a). Compared with other regions and countries, the concentration of DDTs in sediment cores (Zigui, S4) in the TGR was lower (e.g. the concentration of DDTs in the sediment cores of Chaohu Basin, China (0.176–16.534 ng/g) [54], Daya Bay, China [55], and the Sunderban Wetland sediment cores, India [56]). DDT concentration was first observed after mid-1980s (sediment core depth: 8–9 m) and reached its highest concentration in the 2010s (sediment core depth: 1–3 m) (Fig. 3a), which was consistent with the use of pesticides in China. DDT pesticides have been employed in China since the 1950s; from 1960 to 1980, DDT pesticides were used in China. The production and use of DDT accounted for >50 % of the total pesticide production in China [57]. In 1983, China began to completely ban DDT. However, from mid-1990s to mid-2000s, DDT concentrations also increased (sediment core depth: 4–6 m), possibly due to the use of a new DDT ((triclodicarbocide)-containing insecticides) to control mites and destroy mite eggs [54]. With stringent control measures, no DDTs were detected after 2010, fostering remarkable pollution prevention.

(2) PCBs

The concentration of ∑PCBs in the sediment core was ND–11.39 ng/g (Fig. 3b); it reached its peak in the early 1930s (sediment core depth: 20–21 m), possibly because PCBs were commercially manufactured since 1929. Various power capacitors containing PCBs

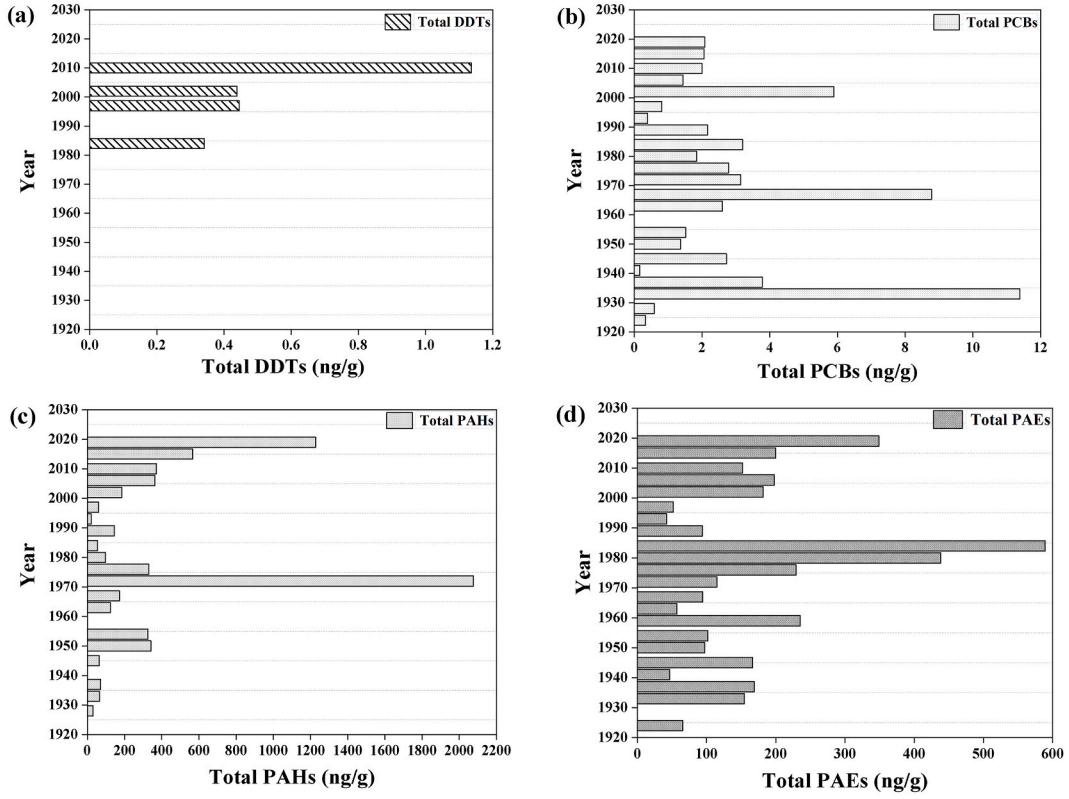

Fig. 3. Concentration distributions of ∑DDTs, ∑PCBs, ∑PAHs and ∑PAEs determined at the research sites.

were introduced in China via international imports, considerably increasing the PCB concentration [58]. Subsequently, PCB concentration decreased and showed a brief gap in the 1950s. However, it sharply increased in the 1960s and 1970s (sediment core depth: 13–14 m). China likely started producing PCB-containing capacitors in 1965. However, as their initial production and management process was chaotic, PCB emissions were high [58]. From the mid-1970s to the end of the 1990s (sediment core depth: 6–12 m), the PCB concentration decreased because most factories in China stopped the production of PCBs in 1974 until it was completely stopped in the early 1980s. However, until the end of the 1990s, large amounts of electrical equipment containing PCBs were still used in China [59]. PCB concentrations increased in the early 2000s (sediment core depths of 3–4 m), consistent with findings in sediment cores from Yangtze River Estuary and the adjacent East China Sea. This was possibly because e-waste recycling activities in some cities generated new sources of PCBs [60]. PCB concentrations decreased from the mid-2000s (sediment core depth: 2–3 m) and stabilised in the 2010–2020s (sediment core depth: 0–3 m), partly due to the Chinese government's ban on e-waste imports and measures to control pollution [60]. Furthermore, the sediment core was analysed to determine the composition of PCBs (Fig. 4). Among the eighteen analysed PCBs, twelve were detected: of which there were tetrachlorobiphenyls (Tetra-PCBs), including PCB52, PCB81 and PCB77; pentachlorobiphenyls (Penta-PCBs), including PCB101 and PCB105; hexachlorobiphenyls (Hexa-PCBs), including PCB138, PCB153, PCB167, PCB156, PCB157 and PCB169, and heptachlorobiphenyls (Hepta-PCBs), including PCB180.

The concentrations of Tetra-PCBs (ND–6.27 ng/g) and Hexa-PCBs (ND–8.18 ng/g) were the maximum. Percentage contribution analysis (Fig. S2) revealed that during the study period (1924–2019), the concentrations of Tetra-PCBs and Hexa-PCBs were ND–71.38 % (mean: 42.59 %) and ND–84.93 % (mean: 51.56 %), respectively. PCB52 and PCB169 accounted for the largest proportions in Hexa-PCBs and Hexa-PCBs, respectively.

The changes in PCB profile at different sediment depths reflected possible sources at different time periods (Figs. and Fig. 4). In the 1920s–1940s (sediment core depth: 19–22 m) and 1990–2010s (sediment core depth: 3–5 m), the proportion of Hexa-PCBs was significantly higher than that of Tetra-PCBs. PCB169 (a typical representative of Hexa-PCBs) was one of the most abundant PCB homologues released from secondary aluminium and copper metallurgies; therefore, PCBs might have originated from the manufacturing industry during the time [25]. After PCBs were produced in China in 1960s–1970s (sediment core depth: 10–13 m) and mid-2010s–2020s (sediment core depth: 0–2 m), the proportion of Tetra-PCBs was relatively high. On one hand, it might be the input of industrial wastewater [61]; on the other hand, the long half-life (15 years) of PCB52 (a typical representative of Tetra-PCBs) might also have a certain impact [62].

(3) PAHs

PAHs typically enter the environment through forest fires, volcanic eruptions, biomass burning and vehicle exhaust [63]. Herein, PAH concentration in the sediment core was ND–2075.20 ng/g; the results are presented in Fig. 3c. In 1960s–1970s (sediment core depth: 12–15 m), China underwent rapid industrialisation, and large amounts of forest wood were burned as fuel for steel production, increasing the PAH concentration [64]. Within the scope of this research, the concentration of PAHs began to increase sharply after the 1970s and reached its maximum at 2075.20 ng/g. This trend was in line with the development in the region at that time. The rapid industrialisation and urbanisation increased the energy consumption, and PAHs were primarily generated owing to such natural, agricultural and human activities. In 2000–2020s (sediment core depth: 0–3 m), the PAH concentration continued to increase, possibly due to economic growth and the resulting automobile exhaust emissions [65].

Moreover, the specific compositions of PAHs and their isomer ratios in each sample were analysed to differentiate between potential origins [66,67]. When the Ant/(Ant + Phe) ratio was <0.1, PAHs were mainly derived from petroleum sources. When the ratio was >0.1, PAHs were primarily derived from combustion sources [66]. When the Fla/(Fla + Pyr) ratio was <0.4, PAHs were mainly derived from petroleum. When the Fla/(Fla + Pyr) ratio was between 0.4 and 0.5, PAHs were derived from the combustion of liquid fossil fuels (vehicles and crude oil). When the Fla/(Fla + Pyr) ratio was >0.5, PAHs were derived from the combustion of biofuels such as coal, grass and wood [67]. When the BaA/(BaA + Chr) ratio was <0.2, petroleum was the primary source of PAHs, the combustion source was >0.35 and the mixed source was between 0.2 and 0.35 [66].

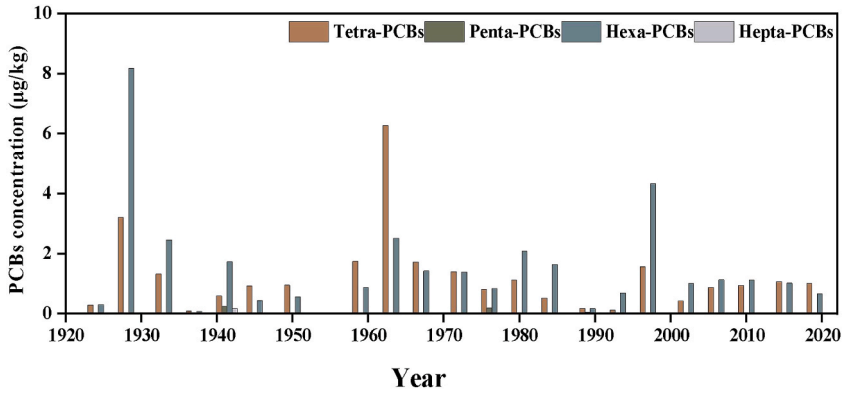

Fig. 4. Composition distribution of PCBs in the sediment core in the TGR.

The changes in PAH profile based on different sediment depths reflected the possible sources in different periods (Fig. 5). In the monitored data, the Ant/(Ant + Phe) ratio was >0.1 and the BaA/(BaA + Chr) ratio was >0.35 at most sampling points. This shows that the PAHs were primarily obtained from a combustion source. Further analysis showed that the Fla/(Fla + Pyr) ratios in most sampling sites were >0.5, indicating that the combustion of grass, wood and coal significantly contributes to PAHs in this particular region [68]. However, the Fla/(Fla + Pyr) ratio in some sampling sites was between 0.4 and 0.5, indicating that the oil source also made a certain contribution. Analysis of the overall source distribution showed that the majority of PAHs in sediments was obtained from the combustion of biomass and coal, with petroleum combustion emerging as the subsequent source.(see Fig. 6)

The primary contributor to PAHs in the TGR was biomass combustion, encompassing activities such as household cooking and burning of crop straw in rural regions. In addition, local petrochemical industries, transportation vehicles (predominantly gasoline combustion), agricultural machineries (primarily diesel combustion) and long-range atmospheric transport play a role in the emission of PAHs derived from petroleum combustion [68]. In recent years, PAH concentrations have continuously increased (Fig. 3c). To address this issue, the adoption of clean-production methods using new energy sources such as photovoltaic and nuclear powers. Moreover, efforts should be made to reduce biomass combustion from coal, petroleum, farmland grass and wood, as well as to control traffic-related oil and gas emissions [69,70].

4.1.2. EDCs

Compared with POPs (DDTs, PCBs and PAHs), EDCs such as PAEs (DBP and DEHP) and HMs (Pb, Cd and Hg) were found in higher concentration and detection frequency in the sediment cores of the TGR.

The vertical distribution of PAEs (Fig. 3d) showed that the concentration of PAEs gradually increased from mid-1960 to mid-1980 (sediment core depth: 9–13 m) and reached its peak in 1984 (589.2 ng/g), possibly due to the rapid development of industrialisation. Particularly in the mid-to-late 1980s, numerous rural industries emerged in China. However, substantial amounts of PAEs were emitted because of outdated equipment and technology, resulting in a peak ΣPAE concentration around 1980s [71]. Notably, the PAE concentration substantially fluctuated in 1980s and 1990s, possibly due to floods [71] or the industrial wastewater control laws and regulations implemented in the early 1990s [72]. Between 2000s and 2020s (specifically, a sediment core depth of 0–3 m), the overall concentration of PAEs noticeably increased due to factors such as population growth, urbanisation and industrial and agricultural developments, such as building products, plastic production and processing, paint and coating manufacturing, ink manufacturing, car products, food packaging and medical devices [73].

The vertical concentration distributions of DBP and DEHP are shown in Fig. S3. The DEHP concentration sharply increased in the 1980s, similar to ΣPAEs, because DEHP was the primary contributor to PAEs. DBP gradually increased from the late 2000s to the 2020s (sediment core depth: 0–3 m) and peaked in 2019 (220.5 ng/g), possibly due to the continued discharge of industrial wastewater [72].

The vertical concentration distribution of HMs is shown in Fig. 6 and S4. In the early stage, the concentrations of Cd and Hg were relatively stable but significantly decreased in 1960s, possibly owing to the slow social development and decline in industrial capacity [74]. From 1970 to 1990s (sediment core depth: 7–12 m), the concentration of HMs was stable and low compared to those in other years. Cd sharply increased in the early 2000s, reaching its peak, possibly due to serious Cd pollution caused by human activities (including mining development and urbanisation) [75]. The main sources of Pb included agricultural non-point source runoff and industrial sewage; however, Pb concentration increased in the past two years, indicating that human activities were still affecting the deposition of HMs. For example, Zhongxian County is located in the central part of Chongqing and is rich in mineral resources, including coal, sulphurous iron ore, copper, lead, alluvial gold, etc. Therefore, it can be assumed that industrial activities such as mining and smelting are an important source of heavy metal contamination in this tributary. HM pollution must be controlled [76].

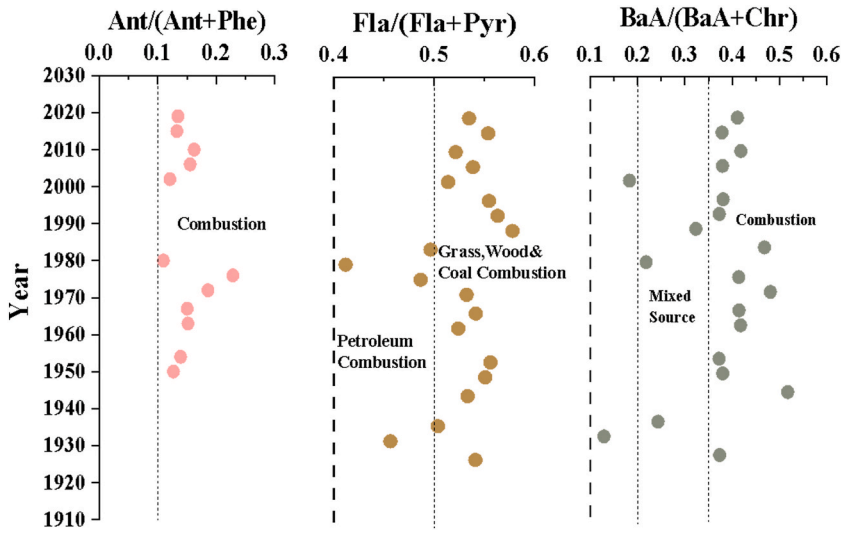

Fig. 5. Analysis of PAHs ratios in the sediment core of the TGR.

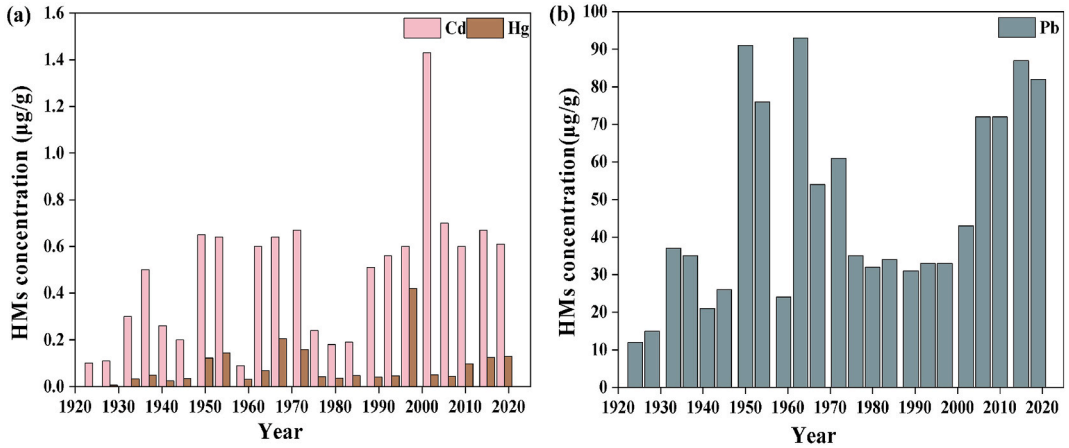

Fig. 6. Composition of Cd, Hg and Pb in the sediment core of the TGR.

4.1.3. Distance–decay relations

To further analyse the distributions of POPs and EDCs in the sediment core, the vertical DDRs of POPs and EDCs were determined using the vegan package in R programming (Version 3.6.3). As shown in Fig. 7, the dissimilarity matrices of POPs and EDCs significantly increased with increasing depth distance (POPs: $r = 0.19$, $p = 0.025$; EDCs: $r = 0.20$, $p = 0.032$), i.e. the similarity of POPs and EDCs significantly decreased with increasing depth distance in the sediment core. Therefore, a DDR exists in the vertical spatial distribution of POPs and EDCs, which is commonly observed in natural environments [77].

4.2. Effects of environmental factors

4.2.1. Correlation analysis

The correlations between POPs (DDT, PCBs and PAHs), EDCs (PAEs and HMs) and other environmental factors (nitrogen and phosphorus) are shown in Fig. 8a. A significant correlation existed between DDT and NO_2 ($r = 0.786$, $p < 0.01$). In addition, significant correlations existed between PAHs, Pb, TN and NH_3–N. The correlation coefficients of PAH–TN, PAH–NH_3–N, Pb–TN and Pb–NH_3–N were 0.724 ($p < 0.01$), 0.509 ($p < 0.05$), 0.897 ($p < 0.01$) and 0.863 ($p < 0.01$), respectively. A significant correlation existed between PAHs and Pb ($r = 0.468$, $p < 0.01$). Nitrogen elements (TN and NH_3–N) were primarily obtained from urban and industrial wastewater and agricultural land, indicating that the sources of PAHs and Pb were closely related to human activities [78].

Owing to long-term accumulation, sediments gradually release phosphorus into water and cause endogenous pollution. Total phosphorus (TP) represents the pollution degree and the release risk of phosphorus in sediments, calcium-bound phosphorus (HCl–P) gets easily deposited in organisms and their bioutilisation is difficult. However, iron- or manganese-bound phosphorus (NaOH–P) is easily decomposed and bioutilised. Therefore, the correlation between HCl–P, NaOH–P and TP in sediments was analysed. The results showed that HCl–P, NaOH–P and TP were strongly correlated; however, POPs and EDCs exhibited a weak correlation, indicating that they were not affected by phosphorus (Fig. 8a).

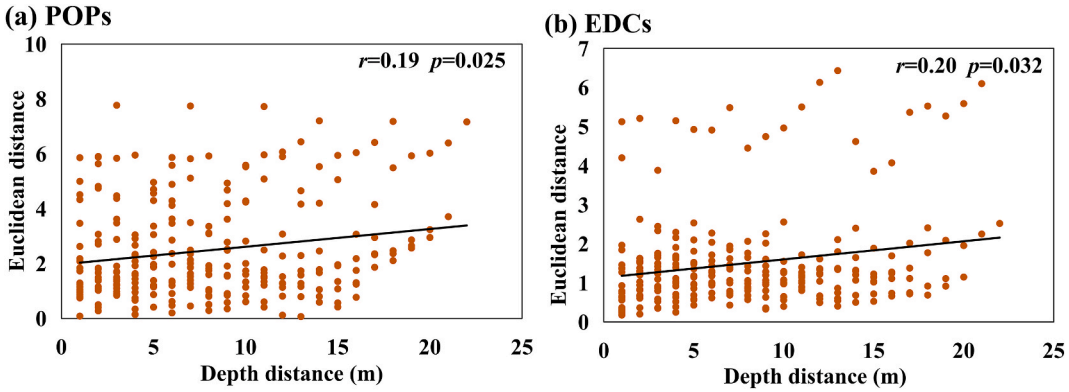

Fig. 7. Changes in the dissimilarity of (a) POPs and (b) EDCs (Euclidean distance) between different depths of sediment core along the depth distance. *r* and *p* indicate the Mantel correlation coefficient and significance of a relationship.

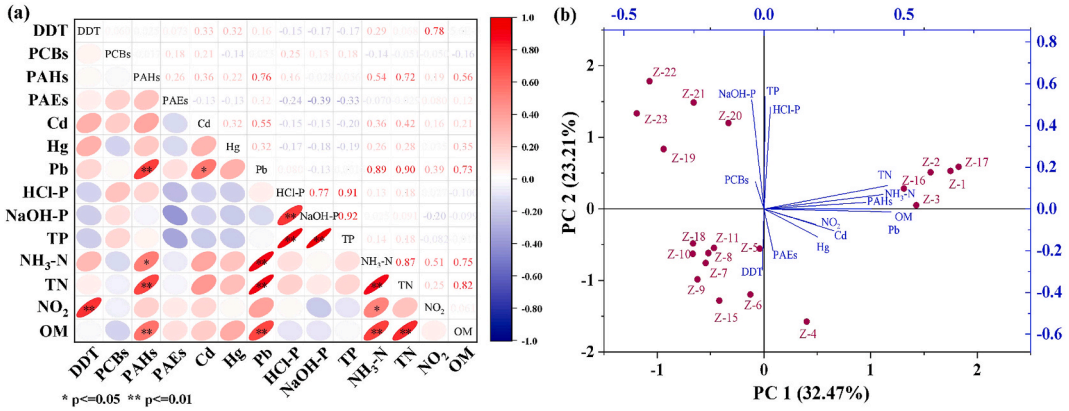

Fig. 8. Correlation analysis (a) and PCA results (b) of POPs, EDCs and other environmental factors in the sediment core.

4.2.2. *Principal component analysis*

The principal-component-analysis (PCA) double plot is shown in Fig. 8b. The variance percentages of the first and second axes were 32.47 % and 23.21 %, respectively. OM, TN, TP, HCl–P, NH_3–N and PAHs exhibited a robust positive correlation with the first axis. In contrast, TP, HCl–P, NaOH–P and PCBs displayed a strong positive correlation with the second axis, whereas DDT, PAEs, Pb, Cd, Hg and NO_2 demonstrated a significant negative correlation with the second axis. The sediment core samples significantly varied (Fig. 8b). The analysis of the correlation between sampling sites and environmental factors revealed that Z-5 and Z-6 were primarily affected by DDT and Z-3 and Z-16 were mainly affected by TN, NH_3–N and OM. Z-19–Z-23 were distributed far away from other sampling sites, indicating that the bottom sediments were primarily affected by biogenic elements such as phosphorus (TP, HCl–P and NaOH–P) and less disturbed by organic pollutants. However, other sampling sites were affected by POPs, EDCs and environmental factors (nitrogen and phosphorus) and did not exhibit significant differences.

4.2.3. *VPA*

The effects of nitrogen, phosphorus and OM on the distribution patterns of POPs (DDT, PCBs and PAHs) and EDCs (PAEs and HMs) were assessed via VPA, wherein the unique and shared interpretation rates of POPs and EDCs were calculated for TN, TP and OM. The total-interpretation rate of POPs by environmental factors was 67.2 %, among which the single-interpretation rate of TN was the highest (48.0 %) and posed a significant effect ($F = 18.8$, $P = 0.003$). OM also had a significant effect on POPs ($F = 6.79$, $P = 0.02$), with a separate interpretation rate of 15.6 %, whereas the interpretation rate of TP to POPs was negligible (Fig. 9a). This showed that POPs were mainly affected by TN and OM, whereas the influence of TP was very limited. The total-interpretation rate of environmental factors to EDCs was only 12.5 %, and the influence of each environmental factor was not significant, indicating that EDCs were negligibly affected by TN, TP and OM (Fig. 9b).

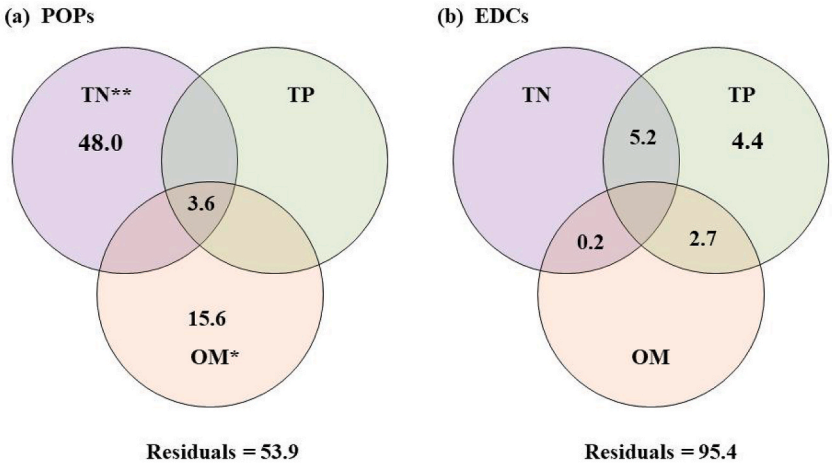

Fig. 9. Venn diagram showing the unique and shared contributions of TN, TP and OM to (a) POPs and (b) EDCs in the sediment core. Values < 0 are not shown and residuals represent unexplained fractions. * indicates significance, *P < 0.05, **P < 0.01, ***P < 0.001.

4.3. Ecological risk assessment

Based on the recorded pollutant levels in surface sediments at various sampling locations and sediment core at different depths in Zigui in the TGR (Table S12), the regulatory standards set by the United States' National Oceanic and Atmospheric Administration and the Canadian Council of Ministers of the Environment were implemented [79]. In summary, the ecological risk of POPs and EDCs in typical sections and sediment cores of the TGR were low.

Furthermore, the ecological risk of PAHs can be assessed by calculating the risk quotient (RQ) based on a previously described method [80]. This method involves quantifying the potential adverse effects of PAHs on the environment and comparing them to appropriate threshold levels (Tables S13 and S14). The RQ_{NCs} and RQ_{MPCs} of each PAH monomer were calculated using the formulas $RQ_{NCs} = C_{PAHs}/C_{QV(NCs)}$ and $RQ_{MPCs} = C_{PAHs}/C_{QV(MPCs)}$, respectively, where $C_{QV(NCs)}$ is the concentration standard that can be ignored and $C_{QV(MPCs)}$ is the maximum allowable concentration standard. After examining the PAH concentration in the surface sediment from various sampling sites (Table S13), the RQ_{NCs} values of Ace, Chr, BaP and DahA were determined to be < 1. PAHs did not pose any ecological risk, while those of the other PAH monomers (including Nap, Phe, Ant, Fla, Acy, Pyr, BbF, InP, BaA, Flu and BghiP) were at $1 < RQ_{NCs} < 800$ and $RQ_{MPCs} < 1$, indicating a low ecological risk. Further analysis of PAHs in the sediment core in Zigui showed that the RQ_{NCs} of Acy, Chr, BaP and DahA were <1, indicating no ecological risk associated with these PAH monomers. However, other PAH monomers such as Flu, Phe, Ant, Pyr, Fla, BaA, Ace, BbF, InP, Nap and BghiP had RQ_{NCs} values ranging from 1 to 800 and RQ_{MPCs} values of <1, indicating a low ecological-risk level (Table S14).

To assess the ecological risk associated with PCBs in surface sediments at various sampling points and the sediment core in Zigui in the TGR (Table S15), the PERI method [81] was utilised. $C_f^i = C^i/C_n^i$ and $E_r^i = T_i \times C_f^i$, where C^i is the concentration of a single pollutant in the sediment, C_n^i is the concentration of the same pollutant before globalisation (0.1 mg/kg) and T_i is the response parameter of a single pollutant, defined as 40 for PCBs. Using this parameter, E_r^i was calculated for individual PCBs to be well below the limiting threshold of 40, indicating a low potential ecological risk.

The SQGQ method [82] was used for the ecological risk assessment of DDTs (Table S16), the PEL quotient ($PELQ_i$) $= C_i/PEL$, SQGQ $= \sum_{i=1}^{n} PELQi/n$, SQGQ $= \sum_{i=1}^{n} PELQi/n$, where C_i is the concentration of pollutant i, which was measured and compared to the corresponding PEL of 51.7 ng/g [83]. The amount of OCPs is represented by n. The resulting SQGQ value was <0.1, indicating no potential ecological risk.

The ecological risk posed by PAEs and HMs was assessed by calculating RQ [84]: $RQ = C_{(EDC)}/PEL$, where PEL is the possible effect concentration of the corresponding pollutant [85,86]. The RQ of DBP was <1, indicating no ecological risk, whereas that of DEHP was >1, indicating a certain ecological risk (Table S17). For HMs, the RQs of Cd and Hg were <0.01, indicating almost no ecological risk, whereas that of Pb was >1, indicating a certain potential ecological risk (Table S18), which must be addressed.

5. Conclusions

This study focused on the historical deposition and evolution characteristics of POPs (DDTs, PCBs and PAHs) and EDCs (PAEs and HMs) in the typical watersheds of the TGR. Surface sediments in the TGR exhibited higher concentrations of PCBs, PAHs, PAEs and HMs compared with those under the dam because of dam interception as well as industrial and agricultural activities. PAHs were the most widely distributed POPs in the reservoir area, sourced from biomass and coal burning, whereas PAEs, specifically DEHP and DBP, were prominent among EDCs. Pb exhibited the highest concentration among HMs, indicating its origin from human population, urban development and intensified industrial and agricultural practices. The overall ecological risk of POPs and EDCs in the TGR was relatively low, with DEHP and Pb warranting special attention. The vertical-distribution pattern of POPs was primarily influenced by TN and OM, whereas EDCs were minimally affected by these factors. Additionally, a DDR was observed for both POPs and EDCs, indicating a decrease in similarity with increasing sediment core depth. These findings offer valuable insights for environmental planning and management of large-scale watersheds.

In recent years, the concentration of certain pollutants in PAE and HM has shown an upward trend, sparking our utmost concern. To address this observed trend, we have proposed several mitigation measures. Controlling the source is crucial, and we should aim to reduce the use of PAE and heavy metals, or seek alternative materials to replace them. Additionally, environmental monitoring and ecological restoration hold utmost importance. We need to strengthen monitoring efforts and formulate corresponding ecological restoration measures. By doing so, we can more effectively tackle this environmental issue.

Data availability

Data relevant to this study are not deposited in publicly available repositories. Data will be made available upon request.

Funding statement

This work was supported by the National Natural Science Foundation of China (No. 52179057), the Natural Science of Hubei Province for Distinguished Young Scholars (No. 2023AFA056) and the State-level Public Welfare Scientific Research Institutes Basic Scientific Research Business Project of China (No. CKSF2023337/SH).

CRediT authorship contribution statement

Lei Dong: Writing – original draft, Supervision, Methodology, Investigation, Conceptualization. **Yueqi Cao:** Writing – original draft, Investigation, Data curation. **Xiong Pan:** Investigation, Data curation. **Li Lin:** Writing – review & editing, Validation, Resources, Funding acquisition. **Xiaohe Luo:** Writing – review & editing, Visualization. **Nima Dunzhu:** Investigation, Data curation. **Jiancheng Hu:** Software.

Declaration of competing interest

The authors declare that they have no known competing financial interests or personal relationships that could have appeared to influence the work reported in this paper.

Acknowledgements

We would like to thank Enago (https://www.enago.cn) for English language editing.

Appendix A. Supplementary data

Supplementary data to this article can be found online at https://doi.org/10.1016/j.heliyon.2024.e32920.

References

[1] X. Ren, G. Zeng, L. Tang, J. Wang, J. Wan, Y. Liu, J. Yu, H. Yi, S. Ye, R. Deng, Sorption, transport and biodegradation – an insight into bioavailability of persistent organic pollutants in soil, Sci. Total Environ. 610–611 (2018) 1154–1163, https://doi.org/10.1016/j.scitotenv.2017.08.089.
[2] B. Güzel, O. Canlı, Pollution profile, source identification, and risk assessments of persistent organic pollutants (POPs) and toxic elements in the sediments of one of the water supply areas (Sultanbahçedere lake) to Istanbul, Türkiye, Reg. Stud. Mar. Sci. 66 (2023) 103146, https://doi.org/10.1016/j.rsma.2023.103146.
[3] S. Khan, Mu Naushad, M. Govarthanan, J. Iqbal, S.M. Alfadul, Emerging contaminants of high concern for the environment: current trends and future research, Environ. Res. 207 (2022) 112609, https://doi.org/10.1016/j.envres.2021.112609.
[4] Y. Chen, J. Yang, B. Yao, D. Zhi, L. Luo, Y. Zhou, Endocrine disrupting chemicals in the environment: environmental sources, biological effects, remediation techniques, and perspective, Environ. Pollut. 310 (2022) 119918, https://doi.org/10.1016/j.envpol.2022.119918.
[5] C. Teodora Ciucure, E.-I. Geana, C. Lidia Chitescu, S. Laurentiu Badea, R. Elena Ionete, Distribution, sources and ecological risk assessment of polycyclic aromatic hydrocarbons in waters and sediments from Olt River dam reservoirs in Romania, Chemosphere 311 (2023) 137024, https://doi.org/10.1016/j.chemosphere.2022.137024.
[6] B. Güzel, O. Canlı, E. Aslan, Spatial distribution, source identification and ecological risk assessment of POPs and heavy metals in lake sediments of Istanbul, Turkey, Mar. Pollut. Bull. 175 (2022) 113172, https://doi.org/10.1016/j.marpolbul.2021.113172.
[7] D. Ciszewski, E. Łokas, Application of 239,240 Pu, 137 Cs and heavy metals for dating of river sediments, Geochronometria 46 (2019) 138–147, https://doi.org/10.1515/geochr-2015-0111.
[8] Z. Yang, Z. Tang, Z. Shen, J. Niu, H. Wang, One-hundred-year sedimentary record of polycyclic aromatic hydrocarbons in urban lake sediments from Wuhan, Central China, water air, Soil Pollut 217 (2011) 577–587, https://doi.org/10.1007/s11270-010-0611-x.
[9] K.K. Singh, S. Vasudevan, Reconstruction of sedimentation rates based on the chronological framework of Lake Pykara, Tamil Nadu, India, Environ. Monit. Assess. 193 (2021) 428, https://doi.org/10.1007/s10661-021-09200-0.
[10] B. Zhou, K. Zhu, Y. Bi, B. Henkelmann, S. Bernhöft, W. Mi, K.-W. Schramm, Distribution pattern of dioxins in sediment cores from the Xiangxi River, a tributary of three Gorges reservoir, China, Water 15 (2023) 57, https://doi.org/10.3390/w15010057.
[11] R.L. Franklin, D.I.T. Fávaro, S.R. Damatto, Trace metal and rare earth elements in a sediment profile from the Rio Grande Reservoir, São Paulo, Brazil: determination of anthropogenic contamination, dating, and sedimentation rates, J. Radioanal. Nucl. Chem. 307 (2016) 99–110, https://doi.org/10.1007/s10967-015-4107-4.
[12] K.E. Juracek, A.C. Ziegler, Estimation of sediment sources using selected chemical tracers in the Perry lake basin, Kansas, USA, Int. J. Sediment Res. 24 (2009) 108–125, https://doi.org/10.1016/S1001-6279(09)60020-2.
[13] L. Fontana, P.A. Ferreira, R.F. Benassi, A.A. Baldovi, R.C.L. Figueira, L.R. Tambosi, A. Calaboni, D.A. Tavares, X. Huang, S.F. Benassi, J.E. de Souza, T.A. de Jesus, Sedimentation rate inferred from 210Pb and 137Cs dating of three sediment cores at Itaipu reservoir (Paraná State, Brazil) the world's second largest hydroelectricity producer, J. Radioanal. Nucl. Chem. 331 (2022) 3571–3589, https://doi.org/10.1007/s10967-022-08380-4.
[14] S.L. Yang, J.D. Milliman, K.H. Xu, B. Deng, X.Y. Zhang, X.X. Luo, Downstream sedimentary and geomorphic impacts of the three Gorges dam on the Yangtze River, Earth Sci. Rev. 138 (2014) 469–486, https://doi.org/10.1016/j.earscirev.2014.07.006.
[15] J. Wang, Y. Bi, G. Pfister, B. Henkelmann, K. Zhu, K.-W. Schramm, Determination of PAH, PCB, and OCP in water from the Three Gorges Reservoir accumulated by semipermeable membrane devices (SPMD), Chemosphere 75 (2009) 1119–1127, https://doi.org/10.1016/j.chemosphere.2009.01.016.
[16] L. Lin, L. Dong, X. Meng, Q. Li, Z. Huang, C. Li, R. Li, W. Yang, J. Crittenden, Distribution and sources of polycyclic aromatic hydrocarbons and phthalic acid esters in water and surface sediment from the Three Gorges Reservoir, J. Environ. Sci. (China) 69 (2018) 271–280, https://doi.org/10.1016/j.jes.2017.11.004.
[17] T. Floehr, B. Scholz-Starke, H. Xiao, J. Koch, L. Wu, J. Hou, A. Wolf, A. Bergmann, K. Bluhm, X. Yuan, M. Roß-Nickoll, A. Schäffer, H. Hollert, Yangtze Three Gorges Reservoir, China: a holistic assessment of organic pollution, mutagenic effects of sediments and genotoxic impacts on fish, J. Environ. Sci. (China) 38 (2015) 63–82, https://doi.org/10.1016/j.jes.2015.07.013.
[18] H. Yang, K. Song, L. Chen, L. Qu, Hysteresis effect and seasonal step-like creep deformation of the Jiuxianping landslide in the Three Gorges Reservoir region, Eng. Geol. 317 (2023) 107089, https://doi.org/10.1016/j.enggeo.2023.107089.
[19] R. Xiang, L. Wang, H. Li, Z. Tian, B. Zheng, Temporal and spatial variation in water quality in the Three Gorges Reservoir from 1998 to 2018, Sci. Total Environ. 768 (2021) 144866, https://doi.org/10.1016/j.scitotenv.2020.144866.
[20] M. Tang, Q. Xu, H. Yang, S. Li, J. Iqbal, X. Fu, X. Huang, W. Cheng, Activity law and hydraulics mechanism of landslides with different sliding surface and permeability in the Three Gorges Reservoir Area, China, Eng. Geol. 260 (2019) 105212, https://doi.org/10.1016/j.enggeo.2019.105212.
[21] Q. Lao, G. Liu, X. Zhou, F. Chen, S. Zhang, Sources of polychlorinated biphenyls (PCBs) and dichlorodiphenyltrichloroethanes (DDTs) found in surface sediment from coastal areas of Beibu Gulf: a reflection on shipping activities and coastal industries, Mar. Pollut. Bull. 167 (2021) 112318, https://doi.org/10.1016/j.marpolbul.2021.112318.

[22] B. Dinç, A. Çelebi, G. Avaz, O. Canlı, B. Güzel, B. Eren, U. Yetis, Spatial distribution and source identification of persistent organic pollutants in the sediments of the Yeşilırmak River and coastal area in the Black Sea, Mar. Pollut. Bull. 172 (2021) 112884, https://doi.org/10.1016/j.marpolbul.2021.112884.

[23] O. Canlı, K. Çetintürk, B. Güzel, A comprehensive assessment, source input determination and distribution of persistent organic pollutants (POPs) along with heavy metals (HMs) in reservoir lake sediments from Çanakkale province, Türkiye, Environ. Geochem. Health 45 (2023) 3985–4006, https://doi.org/10.1007/s10653-023-01480-4.

[24] M.F. Sari, F. Esen, B. Cetin, Concentration levels, spatial variations and exchanges of polychlorinated biphenyls (PCBs) in ambient air, surface water and sediment in Bursa, Türkiye, Sci. Total Environ. 880 (2023) 163224, https://doi.org/10.1016/j.scitotenv.2023.163224.

[25] X. Wang, H. Xu, Y. Zhou, C. Wu, P. Kanchanopas-Barnette, Spatial distribution and sources of polychlorinated biphenyls in surface sediments from the zhoushan archipelago and xiangshan harbor, East China Sea, Mar. Pollut. Bull. 105 (2016) 385–392, https://doi.org/10.1016/j.marpolbul.2016.02.022.

[26] S. Gao, J. Chen, Z. Shen, H. Liu, Y. Chen, Seasonal and spatial distributions and possible sources of polychlorinated biphenyls in surface sediments of Yangtze Estuary, China, Chemosphere 91 (2013) 809–816, https://doi.org/10.1016/j.chemosphere.2013.01.085.

[27] Y. Li, T. Jiang, L. Jing, L. Ni, J. Hua, Y. Chen, Characteristics and risk assessment of PCBs in drinking water source reservoirs of the Zhoushan Islands, East China, Lake Reserv, Manag 30 (2014) 273–284, https://doi.org/10.1080/10402381.2014.924606.

[28] N. An, S. Liu, Y. Yin, F. Cheng, S. Dong, X. Wu, Spatial distribution and sources of polycyclic aromatic hydrocarbons (PAHs) in the reservoir sediments after impoundment of Manwan Dam in the middle of Lancang River, China, Ecotoxicol 25 (2016) 1072–1081, https://doi.org/10.1007/s10646-016-1663-5.

[29] B. Güzel, O. Canlı, A. Çelebi, Characterization, source and risk assessments of sediment contaminants (PCDD/Fs, DL-PCBs, PAHs, PCBs, OCPs, metals) in the urban water supply area, Appl. Geochem. 143 (2022) 105394, https://doi.org/10.1016/j.apgeochem.2022.105394.

[30] L.M. Guimarães, E.J. De França, G.N. de Arruda, A.C.R. de Albergaria-Barbosa, Historical inputs of polycyclic aromatic hydrocarbons in the preserved tropical estuary of the Itapicuru River, Bahia, Brazil, Mar. Pollut. Bull. 156 (2020) 111218, https://doi.org/10.1016/j.marpolbul.2020.111218.

[31] Y. Qi, A.A. Owino, V.A. Makokha, Y. Shen, D. Zhang, J. Wang, Occurrence and risk assessment of polycyclic aromatic hydrocarbons in the Hanjiang River Basin and the Danjiangkou reservoir, China, Hum. Ecol. Risk Assess. 22 (2016) 1183–1196, https://doi.org/10.1080/10807039.2016.1147942.

[32] F. Xie, G. Cai, D. Zhang, G. Li, H. Li, B. Xu, J. Zhang, J. Wang, Distribution, source apportionment and risk assessment of polycyclic aromatic hydrocarbons (PAHs) in surface sediments at the basin scale: a Case study in Taihu Basin, China, Bull. Environ. Contam. Toxicol. 110 (2023) 1–6, https://doi.org/10.1007/s00128-022-03670-9.

[33] X. Xu, K. Cui, Y. Chen, X. Chen, Z. Guo, H. Chen, G. Deng, Y. He, Comprehensive insights into the occurrence, source, distribution and risk assessment of polycyclic aromatic hydrocarbons in a large drinking reservoir system, Environ. Sci. Pollut. Res. 29 (2022) 6449–6462, https://doi.org/10.1007/s11356-021-16142-0.

[34] T. Lin, Y. Qin, B. Zheng, Y. Li, Y. Chen, Z. Guo, Source apportionment of polycyclic aromatic hydrocarbons in the Dahuofang Reservoir, Northeast China, Environ. Monit. Assess. 185 (2013) 945–953, https://doi.org/10.1007/s10661-012-2605-1.

[35] C.-W. Fan, T.-N. Yang, S.-J. Kao, Characteristics of sedimentary polycyclic aromatic hydrocarbons (PAHs) in the subtropical Feitsui Reservoir, Taiwan, J. Hydrol 391 (2010) 217–222, https://doi.org/10.1016/j.jhydrol.2010.07.020.

[36] W.-H. Li, Y.-Z. Tian, G.-L. Shi, C.-S. Guo, X. Li, Y.-C. Feng, Concentrations and sources of PAHs in surface sediments of the Fenhe reservoir and watershed, China, Ecotoxicol. Environ. Saf. 75 (2012) 198–206, https://doi.org/10.1016/j.ecoenv.2011.08.021.

[37] M. Qiao, W. Qi, H. Liu, J. Qu, Oxygenated, nitrated, methyl and parent polycyclic aromatic hydrocarbons in rivers of Haihe River System, China: occurrence, possible formation, and source and fate in a water-shortage area, Sci. Total Environ. 481 (2014) 178–185, https://doi.org/10.1016/j.scitotenv.2014.02.050.

[38] J. Zhang, L. Cai, D. Yuan, M. Chen, Distribution and sources of polynuclear aromatic hydrocarbons in Mangrove surficial sediments of Deep Bay, China, Mar. Pollut. Bull. 49 (2004) 479–486, https://doi.org/10.1016/j.marpolbul.2004.02.030.

[39] S. Feng, B. Mai, G. Wei, X. Wang, Genotoxicity of the sediments collected from Pearl River in China and their polycyclic aromatic hydrocarbons (PAHs) and heavy metals, Environ. Monit. Assess. 184 (2012) 5651–5661, https://doi.org/10.1007/s10661-011-2369-z.

[40] Y. Liu, Y. Tang, Y. He, H. Liu, S. Tao, W. Liu, Riverine inputs, spatiotemporal variations, and potential sources of phthalate esters transported into the Bohai Sea from an urban river in northern China, Sci. Total Environ. 878 (2023) 163253, https://doi.org/10.1016/j.scitotenv.2023.163253.

[41] Y. Liu, Y. He, J. Zhang, C. Cai, F. Breider, S. Tao, W. Liu, Distribution, partitioning behavior, and ecological risk assessment of phthalate esters in sediment particle-pore water systems from the main stream of the Haihe River, Northern China, Sci. Total Environ. 745 (2020) 141131, https://doi.org/10.1016/j.scitotenv.2020.141131.

[42] B.-T. Zhang, Y. Gao, C. Lin, T. Liu, X. Liu, Y. Ma, H. Wang, Spatial distribution of phthalate acid esters in sediments and its relationships with anthropogenic activities and environmental variables of the Jiaozhou Bay, Mar. Pollut. Bull. 155 (2020) 111161, https://doi.org/10.1016/j.marpolbul.2020.111161.

[43] Z. Weizhen, Z. Xiaowei, G. Peng, W. Ning, L. Zini, H. Jian, Z. Zheng, Distribution and risk assessment of phthalates in water and sediment of the Pearl River Delta, Environ. Sci. Pollut. Res. 27 (2020) 12550–12565, https://doi.org/10.1007/s11356-019-06819-y.

[44] M. Bulbul, S. Bhattacharya, Y. Ankit, P. Yadav, A. Anoop, Occurrence, distribution and sources of phthalates and petroleum hydrocarbons in tropical estuarine sediments (Mandovi and Ashtamudi) of western Peninsular India, Environ. Res. 214 (2022) 113679, https://doi.org/10.1016/j.envres.2022.113679.

[45] T. Zhang, Y. Li, Spatial distribution, fractions and risk assessment of five heavy metals in the sediments of Jialing River: a tributary of the Yangtze, Environ. Earth Sci. 79 (2020) 1–12, https://doi.org/10.1007/s12665-020-09216-8.

[46] L. Lin, C. Li, W. Yang, L. Zhao, M. Liu, Q. Li, J.C. Crittenden, Spatial variations and periodic changes in heavy metals in surface water and sediments of the Three Gorges Reservoir, China, Chemosphere 240 (2020) 124837, https://doi.org/10.1016/j.chemosphere.2019.124837.

[47] D. Han, J. Cheng, X. Hu, Z. Jiang, L. Mo, H. Xu, Y. Ma, X. Chen, H. Wang, Spatial distribution, risk assessment and source identification of heavy metals in sediments of the Yangtze River Estuary, China, Mar. Pollut. Bull. 115 (2017) 141–148, https://doi.org/10.1016/j.marpolbul.2016.11.062.

[48] J. Liang, J. Liu, X. Yuan, G. Zeng, X. Lai, X. Li, H. Wu, Y. Yuan, F. Li, Spatial and temporal variation of heavy metal risk and source in sediments of Dongting Lake wetland, mid-south China, J Environ Sci Heal A 50 (2015) 100–108, https://doi.org/10.1080/10934529.2015.964636.

[49] T. Javed, N. Ahmad, A. Mashiatullah, K. Khan, Chronological record, source identification and ecotoxicological impact assessment of heavy metals in sediments of Kallar Kahar Lake, Salt Range-Punjab, Pakistan, Environ. Earth Sci. 80 (2021) 1–18, https://doi.org/10.1007/s12665-021-09764-7.

[50] S. Hua, T. ChangYin, H. DaoYou, W. DaJuan, L. LiKe, Y. Yan, Y. Xia, Effects of Soil Organic Matter on the Accumulation, Availability, and Chemical Speciation of Heavy Metal, vol.34, Journal of Natural Science of Hunan Normal University, 2011, pp. 82–87 (In Chinese).

[51] M. Wang, G. Song, C. Zhang, F. Zhai, W. Wang, Z. Song, Chemical fractionation and risk assessment of surface sediments in Luhun Reservoir, Luoyang city, China, Environ. Sci. Pollut. Res. 27 (2020) 35319–35329, https://doi.org/10.1007/s11356-020-09512-7.

[52] H. Zhao, G. Sun, Z. Li, L. Zhang, X. Feng, X. Li, T. Wu, Total mercury and mercury isotope signatures in reservoir sediment reflecting the landscape changes and agricultural activities in northeast China, Catena 197 (2021) 104983, https://doi.org/10.1016/j.catena.2020.104983.

[53] Z. Zhang, X. Chen, H. Yao, X. Huang, L. Chen, Experimental investigation on tensile strength of jurassic red-bed sandstone under the conditions of water pressures and wet-dry cycles, KSCE J. Civ. Eng. 25 (2021) 2713–2724, https://doi.org/10.1007/s12205-021-1404-z.

[54] L. Kang, Q.-S. He, W. He, X.-Z. Kong, W.-X. Liu, W.-J. Wu, Y.-L. Li, X.-Y. Lan, F.-L. Xu, Current status and historical variations of DDT-related contaminants in the sediments of Lake Chaohu in China and their influencing factors, Environ. Pollut. 219 (2016) 883–896, https://doi.org/10.1016/j.envpol.2016.08.072.

[55] Z. Wang, W. Yan, J. Chi, G. Zhang, Spatial and vertical distribution of organochlorine pesticides in sediments from Daya Bay, South China, Mar. Pollut. Bull. 56 (2008) 1578–1585, https://doi.org/10.1016/j.marpolbul.2008.05.019.

[56] S.K. Sarkar, A. Binelli, C. Riva, M. Parolini, M. Chatterjee, A.K. Bhattacharya, B.D. Bhattacharya, K.K. Satpathy, Organochlorine pesticide residues in sediment cores of sunderban wetland, northeastern part of Bay of bengal, India, and their ecotoxicological significance, Arch. Environ. Contam. Toxicol. 55 (2008) 358–371, https://doi.org/10.1007/s00244-008-9133-6.

[57] C. Hu, Y. Tao, Spatial–temporal occurrence and sources of organochlorine pesticides in the sediments of the largest deep lake (Lake Fuxian) in China, Environ. Sci. Pollut. Res. 30 (2023) 31157–31170, https://doi.org/10.1007/s11356-022-24394-7.

[58] Z. Yang, Z. Shen, F. Gao, Z. Tang, J. Niu, Y. He, Polychlorinated biphenyls in urban lake sediments from wuhan, Central China: occurrence, composition, and sedimentary record, J. Environ. Qual. 38 (2009) 1441–1448, https://doi.org/10.2134/jeq2008.0111.

[59] Q.Y. Meng, S.G. Chu, X.B. Xu, Research progress on environmental adsorption behavior of polychlorinated biphenyls, Chin. Sci. Bull. 45 (15) (2000) 1572–1583 (In Chinese).
[60] H. Yang, S. Zhuo, B. Xue, C. Zhang, W. Liu, Distribution, historical trends and inventories of polychlorinated biphenyls in sediments from Yangtze River Estuary and adjacent East China Sea, Environ. Pollut. 169 (2012) 20–26, https://doi.org/10.1016/j.envpol.2012.05.003.
[61] X. Wang, B. Xi, S. Huo, L. Deng, Q. Li, H. Pan, J. Zhang, H. Liu, Polychlorinated biphenyls residues in surface sediments of the eutrophic Chaohu Lake (China): characteristics, risk, and correlation with trophic status, Environ. Earth Sci. 71 (2014) 849–861, https://doi.org/10.1007/s12665-013-2487-8.
[62] W. Wang, J. Bai, G. Zhang, J. Jia, X. Wang, X. Liu, B. Cui, Occurrence, sources and ecotoxicological risks of polychlorinated biphenyls (PCBs) in sediment cores from urban, rural and reclamation-affected rivers of the Pearl River Delta, China, Chemosphere 218 (2019) 359–367, https://doi.org/10.1016/j.chemosphere.2018.11.046.
[63] Y. He, X. Wang, Z. Zhang, Polycyclic aromatic hydrocarbons (PAHs) in a sediment core from Lake Taihu and their associations with sedimentary organic matter, J. Environ. Sci. (China) 129 (2023) 79–89, https://doi.org/10.1016/j.jes.2022.09.013.
[64] J. Zhang, H. Huang, R. Wang, R. Sun, Historical pollution and source contributions of PAHs in sediment cores from the middle reach of huai river, China, Bull. Environ. Contam. Toxicol. 102 (2019) 531–537, https://doi.org/10.1007/s00128-019-02576-3.
[65] X. Ma, H. Wan, Z. Zhao, Y. Li, S. Li, C. Huang, T. Huang, Z. Zhang, H. Yang, Source analysis and influencing factors of historical changes in PAHs in the sediment core of Fuxian Lake, China, Environ. Pollut. 288 (2021) 117935, https://doi.org/10.1016/j.envpol.2021.117935.
[66] Y. Zhu, Y. Yang, M. Liu, M. Zhang, J. Wang, Concentration, distribution, source, and risk assessment of PAHs and heavy metals in surface water from the three Gorges reservoir, China, Hum. Ecol. Risk Assess. 21 (2015) 1593–1607, https://doi.org/10.1080/10807039.2014.962315.
[67] B. Ambade, S.S. Sethi, M.R. Chintalacheruvu, Distribution, risk assessment, and source apportionment of polycyclic aromatic hydrocarbons (PAHs) using positive matrix factorization (PMF) in urban soils of East India, Environ. Geochem. Health 45 (2023) 491–505, https://doi.org/10.1007/s10653-022-01223-x.
[68] J. Feng, M. Liu, J. Zhao, P. Hu, F. Zhang, J.-H. Sun, Historical trends and spatial distributions of polycyclic aromatic hydrocarbons in the upper reach of the Huai River, China: evidence from the sedimentary record, Appl. Geochem. 103 (2019) 59–67, https://doi.org/10.1016/j.apgeochem.2019.02.012.
[69] B. Ambade, A. Kumar, M. Latif, Emission sources, Characteristics and risk assessment of particulate bound Polycyclic Aromatic Hydrocarbons (PAHs) from traffic sites. https://doi.org/10.21203/rs.3.rs-328364/v1, 2021.
[70] B. Ambade, T.K. Sankar, L.K. Sahu, U.C. Dumka, Understanding sources and composition of black carbon and PM2.5 in urban environments in East India, Urban Science 6 (2022) 60, https://doi.org/10.3390/urbansci6030060.
[71] W. Zhang, X. Li, C. Guo, J. Xu, Spatial distribution, historical trend, and ecological risk assessment of phthalate esters in sediment from Taihu Lake, China, Environ. Sci. Pollut. Res. 28 (2021) 25207–25217, https://doi.org/10.1007/s11356-021-12421-y.
[72] B. Wang, B. Huang, W. Jin, Y. Wang, S. Zhao, F. Li, P. Hu, X. Pan, Seasonal distribution, source investigation and vertical profile of phenolic endocrine disrupting compounds in Dianchi Lake, China, J. Environ. Monit. 14 (2012) 1275, https://doi.org/10.1039/c2em10856a.
[73] J. Sun, J. Huang, A. Zhang, W. Liu, W. Cheng, Occurrence of phthalate esters in sediments in Qiantang River, China and inference with urbanization and river flow regime, J. Hazard Mater. 248–249 (2013) 142–149, https://doi.org/10.1016/j.jhazmat.2012.12.057.
[74] B. Chen, D. Fan, W. Li, L. Wang, X. Zhang, M. Liu, Z. Guo, Enrichment of heavy metals in the inner shelf mud of the East China Sea and its indication to human activity, Cont Shelf Res 90 (2014) 163–169, https://doi.org/10.1016/j.csr.2014.04.016.
[75] X. Wang, B. Liu, W. Zhang, Distribution and risk analysis of heavy metals in sediments from the Yangtze River Estuary, China, Environ. Sci. Pollut. Res. 27 (2020) 10802–10810, https://doi.org/10.1007/s11356-019-07581-x.
[76] L. Cao, G.H. Hong, S. Liu, Metal elements in the bottom sediments of the Changjiang Estuary and its adjacent continental shelf of the East China Sea, Mar. Pollut. Bull. 95 (2015) 458–468, https://doi.org/10.1016/j.marpolbul.2015.03.013.
[77] J. Soininen, R. McDonald, H. Hillebrand, The distance decay of similarity in ecological communities, Ecography 30 (2007) 3–12, https://doi.org/10.1111/j.0906-7590.2007.04817.x.
[78] W. Li, S. Lin, W. Wang, Z. Huang, H. Zeng, X. Chen, F. Zeng, Z. Fan, Assessment of nutrient and heavy metal contamination in surface sediments of the Xiashan stream, eastern Guangdong Province, China, Environ. Sci. Pollut. Res. 27 (2020) 25908–25924, https://doi.org/10.1007/s11356-019-06912-2.
[79] W.-J. Shim, S.-H. Hong, Application of a sediment quality index to the masan Bay, korea, Ocean Polar Res. 29 (2007) 367–378, https://doi.org/10.4217/OPR.2007.29.4.367.
[80] D.F. Kalf, T. Crommentuijn, E.J. van de Plassche, Environmental quality objectives for 10 polycyclic aromatic hydrocarbons (PAHs), Ecotoxicol. Environ. Saf. 36 (1997) 89–97, https://doi.org/10.1006/eesa.1996.1495.
[81] L. Hakanson, An ecological risk index for aquatic pollution control.a sedimentological approach, Water Res. 14 (1980) 975–1001, https://doi.org/10.1016/0043-1354(80)90143-8.
[82] T. Combi, M.G. Pintado-Herrera, P.A. Lara-Martín, M. Lopes-Rocha, S. Miserocchi, L. Langone, R. Guerra, Historical sedimentary deposition and flux of PAHs, PCBs and DDTs in sediment cores from the western Adriatic Sea, Chemosphere 241 (2020) 125029, https://doi.org/10.1016/j.chemosphere.2019.125029.
[83] Q. Deng, Y. Wei, W. Huang, Y. Li, C. Peng, Y. Zhao, J. Yang, Z. Xu, X. Wang, W. Liang, Sedimentary evolution of PAHs, POPs and ECs: historical sedimentary deposition and evolution of persistent and emerging organic pollutants in sediments in a typical karstic river basin, Sci. Total Environ. 773 (2021) 144765, https://doi.org/10.1016/j.scitotenv.2020.144765.
[84] V.D. Toan, T.X. Quynh, N.T.L. Huong, Endocrine disrupting compounds in sediment from KimNguu river, Northern area of Vietnam: a comprehensive assessment of seasonal variation, accumulation pattern and ecological risk, Environ. Geochem. Health 42 (2020) 647–659, https://doi.org/10.1007/s10653-019-00399-z.
[85] E.R. Long, D.D. Macdonald, S.L. Smith, F.D. Calder, Incidence of adverse biological effects within ranges of chemical concentrations in marine and estuarine sediments, Environ Manage 19 (1995) 81–97, https://doi.org/10.1007/BF02472006.
[86] A.P. Van Wezel, P. Van Vlaardingen, R. Posthumus, G.H. Crommentuijn, D.T.H.M. Sijm, Environmental risk limits for two phthalates, with special emphasis on endocrine disruptive properties, Ecotoxicol. Environ. Saf. 46 (2000) 305–321, https://doi.org/10.1006/eesa.2000.1930.